

On the strength of stainless steel fillet welds

M. Fortan^a, A. Dejans^b, B. Karabulut^a, D. Debruyne^c & B. Rossi^{a,d}

^a Department of Civil Engineering, KU Leuven, Belgium

Jan Pieter de Nayerlaan 5, Sint-Katelijne-Waver, Belgium.

Email: maarten.fortan@kuleuven.be, burak.karabulut@kuleuven.be

^b Department of Mechanical Engineering, KU Leuven, Belgium

Email: arnout.dejans@kuleuven.be

^c Department of Materials Engineering, KU Leuven, Belgium

Email: dimitri.debruyne@kuleuven.be

^d Department of Engineering Science, University of Oxford, United Kingdom

Emails: barbara.rossi@new.ox.ac.uk

Abstract

This paper describes 24 tests performed on welded specimens made of 3 stainless steel grades: EN 1.4307 (304L) and EN 1.4404 (316L) austenitic grades and EN 1.4062 duplex grade. For each grade, tests were carried out parallel to the weld and along the transverse direction. The austenitic grades were welded using GMAW (MAG), while the duplex grades were welded using Gas Metal Arc Welding (GMAW) and Gas Tungsten Arc Welding (GTAW or TIG). After failure, the fracture surfaces were measured using Digital Image Correlation (DIC) and compared to measurements before testing. The results were compared to 70 experiments on welded stainless steel samples, gathered from the literature. A relatively high scatter was found among the different sources as well as differences between grades and loading directions. A reliability study was then performed in agreement with EN 1990:2002 Annex D on the complete experimental data pool and recommendations for the correlation factor β_w are then provided.

Keywords

Stainless steel welds, experiments, DIC, correlation factor β_w , reliability analysis.

1 Introduction

For almost a century, stainless steel was used in building as cladding since it combines aesthetic appearance, good corrosion resistance and ease of maintenance. Famous examples are the Chrysler building and the Empire State building in New York, where stainless steel has been used for the iconic roofs which are still in outstanding state with only limited maintenance [1], most of the time, limited to washing by the rain. Recently, stainless steels, and especially duplex grades, gained more and more popularity in the construction and transport sectors as load-bearing elements because they are also characterized by excellent mechanical properties. A good corrosion resistance combined with very high strength and ductility for the duplex grades led to an increasing use of this family of stainless steel in structural components in applications such as (pedestrian) bridges, with multiple examples such as the Cala Galdana Bridge in Menorca, the Siena Bridge in Ruffolo or the Millenium Bridge in York [2].

The structural stainless steel components include either open or closed cross-sections which are, most of the time, welded cross-sections. Various studies, such as [3] and [4], show that the weldability of stainless steel is good and that most grades can be welded with all commonly used welding processes, provided that appropriate precautions are taken. For duplex welds, an important feature is the balance between austenite and ferrite in the weld metal, which is achieved by using an over alloyed filler material, and the heat affected zone (HAZ), which is accomplished with a heat input lying in a suitable range. However, research on the strength of stainless steel fillet welds is rather scarce as only 70 experiments were found in the scientific literature [5]-[8]. These studies deal with only two grades of stainless steel and two welding processes, gas tungsten arc welding (GTAW or TIG) and shielded metal arc welding (SMAW or MMA).

In EN 1993-1-8 [9], welds are designed by comparing the Von Mises stress in the weld throat plane to the ultimate strength f_u of the base metal multiplied by a partial safety factor. The resistance is also divided by a correlation factor β_w lower than or equal to 1.0, taking into account the variety of carbon steel grades and their corresponding filler materials. For all stainless steel grades, EN 1993-1-4 [10] prescribes $\beta_w = 1.0$. However, current research, such as [11], suggests that a lower correlation factor

β_w could be used for higher strength carbon steel, the strength of which is comparable to the duplex stainless steel family. In this paper, which was partly published in [12] and [13], experiments were conducted on both duplex and austenitic stainless steel welds. Based on these results, a reliability assessment is made to amend the current correlation factor β_w in EN 1993-1-8 [9] and EN 1993-1-4 [10].

2 EN 1993-1-8 design rules for fillet welds

For the design of fillet welds in EN 1993-1-8 [9], the directional method is used. This method, see equation 1, uses the Von Mises criterion and compares the equivalent stress with the design value of the nominal ultimate strength of the weakest component. Additionally, the normal stress perpendicular to the weld throat plane is limited through equation 2.

$$\sqrt{\sigma_{\perp}^2 + 3(\tau_{\perp}^2 + \tau_{\parallel}^2)} \leq \frac{f_u}{\beta_w \gamma_{M2}} \quad (1)$$

$$\sigma_{\perp} \leq \frac{0.9 f_u}{\gamma_{M2}} \quad (2)$$

where: σ_{\perp} is the normal stress perpendicular to the weld throat plane,
 τ_{\perp} is the shear stress, in the weld throat plane, perpendicular to the weld throat axis,
 τ_{\parallel} is the shear stress, in the weld throat plane, parallel to the weld throat axis,
 f_u is the nominal ultimate strength of the weakest joined part,
 β_w is the correlation factor dependant on the used material,
 γ_{M2} is the safety factor for connections.

When the full throat thickness a can be guaranteed along the entire weld, the whole length of the weld is used in the design. However, for most welds this is not the case for the start and end zones where the length should be reduced with two times the throat thickness.

The effective throat thickness should be taken as the height of the inscribed triangle, measured from the weld root to the outside leg of the triangle. When a deeper penetration can be guaranteed and proven by tests, this extra penetration can be taken into account, as shown in Fig. 1.

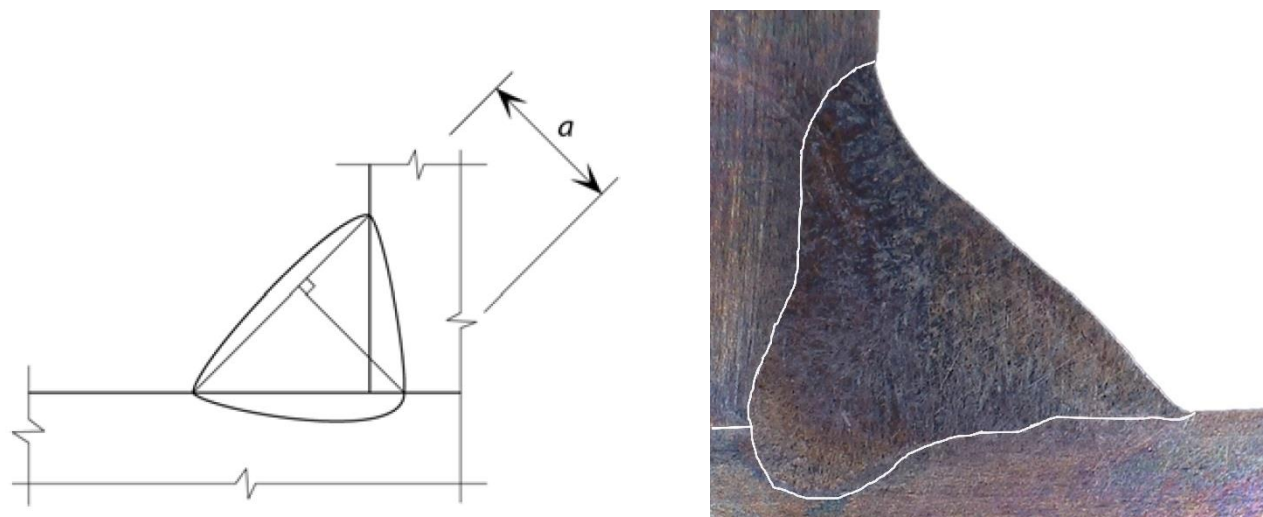


Fig. 1: Throat thickness a for a deep penetration fillet weld (left) and the macroscopic examination of the weld in EN 1.4062 (right).

For the design of welded connections made of stainless steel, EN 1993-1-4 [10], which contains the supplementary rules for stainless steel constructions, refers to the design rules stated in EN 1993-1-8 [9] for carbon steel. The value for the correlation factor β_w should be taken as 1.0 for all stainless steel families, except if tests in accordance with chapter 7 of EN 1993-1-4 [10] justify a lower value. In this paper, the reliability of the directional method with a lower β_w is investigated.

3 Reference research on the strength of stainless steel fillet welds

In the last decades, research on the strength of fillet welds concentrated on high strength steel with different filler materials [11], [14]-[16]. Filler materials with a corresponding strength are difficult to find for very high strength steels and they have a limited ductility. Therefore, it is a common practise to undermatch filler materials for these grades to ensure the desired ductility of the joint, even though it decreases the strength of the weld metal. Consequently, EN 1993-1-12 [17] uses the strength of the filler material in the strength function (equations 1 and 2) while most studies propose an average between the base and filler materials.

More importantly, Kuhlmann et al. [11] propose lowered correlation factors for high strength steels, including S460M which has a similar strength as the duplex stainless steels studied in this paper. The proposed factors depend on the steel grade but also on the loading direction with a different correlation factor for butt welds, transverse fillet welds and longitudinal fillet welds. The study includes experiments on 328 specimens including several joint types and filler materials. The samples were

1 welded in two phases. In the first phase, a semi mechanized gas metal arc welding (GMAW or MAG)
2 process was used, but, to reduce the scatter in the experimental results, a fully mechanized GMAW
3 process was used in the second phase, which resulted in more coherent test results. The difference in
4 strength for the transverse and longitudinal loading directions was also confirmed in [18]-[19] and later
5 for stainless steel in [5]. The fracture angles in [18]-[19] for the transverse welds are considerably
6 lower than the theoretical critical angle of 45° with failure angles around 20° , which could explain the
7 higher strength.

8 The research on the strength of stainless steel fillet welds is quite limited with experiments published
9 in [5]-[8] in contrast to the research on stainless steel weldability, which includes tensile tests and
10 bending tests on butt welds, hardness measurements, impact tests and corrosion tests, see [20]-[29].

11 The report of Stangenberg [5] includes 23 tests on the austenitic grade EN 1.4301 and 23 tests on the
12 duplex grade EN 1.4462 and all specimens were welded using GTAW. The experimental program
13 investigated both longitudinally and transversely loaded fillet welds, collected in Table 1, and
14 concluded that the correlation factor could be reduced for transverse welds but not for longitudinal
15 welds.

16 In 2017, Lee et al. [6] reported more tests on austenitic stainless steel fillet GTAW-welds. Four tests
17 on transverse welds and four tests on the longitudinal strength were performed for EN 1.4301,
18 summarized in Table 2. Moreover, specimens with welds in both longitudinal and transverse direction
19 were studied in this paper and the tests showed that a superposition of both strengths leads to an
20 overestimation of the strength of the combined welded connection.

1 **Table 1: Overview of test results from Stangenberg [5]**

Specimen	Grade	Load direction	Tensile strength base metal MPa	Tensile strength weld metal MPa	Throat thickness mm	Throat length mm	Fracture surface mm ²	Ultimate strength kN
-	-	-	-	-	-	-	-	-
4301P1	EN 1.4301	Longitudinal	659.0	617.0	6.8	54.5	371	277
4301P2	EN 1.4301	Longitudinal	659.0	617.0	6.7	54.4	364	276
4301P3	EN 1.4301	Longitudinal	659.0	617.0	6.9	55.0	380	283
4301P4	EN 1.4301	Longitudinal	659.0	617.0	7.0	55.0	385	277
4301P5	EN 1.4301	Longitudinal	659.0	617.0	6.7	54.7	366	283
4301P7	EN 1.4301	Longitudinal	659.0	617.0	6.8	54.6	371	283
4301P8	EN 1.4301	Longitudinal	659.0	617.0	6.7	54.9	368	287
4301P9	EN 1.4301	Longitudinal	659.0	617.0	6.8	54.8	373	281
4301P10	EN 1.4301	Longitudinal	659.0	617.0	6.9	54.6	377	276
4301P11	EN 1.4301	Longitudinal	659.0	617.0	6.7	54.5	365	290
4301P12	EN 1.4301	Longitudinal	659.0	617.0	6.8	54.9	373	290
4301T2	EN 1.4301	Transverse	659.0	617.0	4.1	55.2	226	307
4301T3	EN 1.4301	Transverse	659.0	617.0	4.0	55.0	220	299
4301T4	EN 1.4301	Transverse	659.0	617.0	4.1	55.1	223	310
4301T5	EN 1.4301	Transverse	659.0	617.0	3.9	54.5	213	262
4301T6	EN 1.4301	Transverse	659.0	617.0	4.2	55.5	233	333
4301T7	EN 1.4301	Transverse	659.0	617.0	4.0	55.1	220	292
4301T8	EN 1.4301	Transverse	659.0	617.0	4.2	55.3	229	309
4301T9	EN 1.4301	Transverse	659.0	617.0	4.1	54.8	222	317
4301T10	EN 1.4301	Transverse	659.0	617.0	4.1	55.4	227	292
4301T11	EN 1.4301	Transverse	659.0	617.0	4.0	54.8	219	311
4301T12	EN 1.4301	Transverse	659.0	617.0	4.2	55.0	228	324
4301T13	EN 1.4301	Transverse	659.0	617.0	4.2	55.5	233	299
4462P1	EN 1.4462	Longitudinal	756.0		6.7	54.8	367	333
4462P2	EN 1.4462	Longitudinal	756.0		6.9	55.5	383	365
4462P3	EN 1.4462	Longitudinal	756.0		6.8	54.5	371	339
4462P4	EN 1.4462	Longitudinal	756.0		6.8	55.0	374	337
4462P5	EN 1.4462	Longitudinal	756.0		6.6	55.3	365	332
4462PL6	EN 1.4462	Longitudinal	756.0		6.7	54.7	366	337
4462PL7	EN 1.4462	Longitudinal	756.0		6.6	54.3	358	330
4462PL8	EN 1.4462	Longitudinal	756.0		6.7	54.9	368	332
4462PL9	EN 1.4462	Longitudinal	756.0		6.8	55.2	375	338
4462PL10	EN 1.4462	Longitudinal	756.0		6.8	55.3	376	361
4462PL11	EN 1.4462	Longitudinal	756.0		6.9	54.8	378	364
4462T1	EN 1.4462	Transverse	756.0		4.1	55.5	228	405
4462T2	EN 1.4462	Transverse	756.0		4.2	54.5	226	404
4462T3	EN 1.4462	Transverse	756.0		4.0	55.2	218	405
4462T4	EN 1.4462	Transverse	756.0		4.2	55.6	234	401
4462T5	EN 1.4462	Transverse	756.0		4.1	54.7	224	403
4462T6	EN 1.4462	Transverse	756.0		4.2	55.5	230	405
4462T7	EN 1.4462	Transverse	756.0		4.2	55.9	235	406
4462T8	EN 1.4462	Transverse	756.0		4.1	56.0	230	403
4462T9	EN 1.4462	Transverse	756.0		4.0	54.6	218	393
4462T10	EN 1.4462	Transverse	756.0		4.2	55.5	230	396
4462T11	EN 1.4462	Transverse	756.0		4.1	55.8	226	405
4462T12	EN 1.4462	Transverse	756.0		4.1	56.1	230	402

2 **Table 2: Overview of test results from Lee et al. [6]**

Specimen	Grade	Load direction	Tensile strength base metal MPa	Tensile strength weld metal MPa	Throat thickness mm	Throat length mm	Fracture surface mm ²	Ultimate strength kN
-	-	-	-	-	-	-	-	-
TFW40-1	EN 1.4301	Transverse	693	574	1.68	40	67	116
TFW40-2	EN 1.4301	Transverse	693	574	1.81	40	72	133
TFW80-1	EN 1.4301	Transverse	693	574	1.84	80	147	242
TFW80-2	EN 1.4301	Transverse	693	574	1.85	80	148	268
LFW40-1	EN 1.4301	Longitudinal	693	574	1.74	40	70	193
LFW40-2	EN 1.4301	Longitudinal	693	574	1.86	40	74	192
LFW80-1	EN 1.4301	Longitudinal	693	574	1.90	80	152	393
LFW80-2	EN 1.4301	Longitudinal	693	574	1.85	80	148	375

In [7], an experimental programme on duplex welds in grade EN 1.4462 is reported by Yang et al (Table 3). All specimens were welded manually with the SMAW-process. Both in the transverse and the longitudinal direction, the experimental results reveal a high degree of conservativeness to the current design rules.

Table 3: Overview of test results from Yang et al. [7]

Specimen	Grade	Load direction	Tensile strength base metal	Tensile strength weld metal	Throat thickness	Throat length	Fracture surface	Ultimate strength
-	-	-	MPa	MPa	mm	mm	mm ²	kN
L6-1	EN 1.4462	Longitudinal	755	847	4.89	50.57	247	632
L6-2	EN 1.4462	Longitudinal	755	847	4.88	50.09	244	605
L6-3	EN 1.4462	Longitudinal	755	847	4.62	50.06	231	592
L6-4	EN 1.4462	Longitudinal	755	847	4.33	50.41	218	551
L6-5	EN 1.4462	Longitudinal	755	847	4.88	50.35	246	626
T6-1	EN 1.4462	Transverse	755	847	4.78	51.18	244	469
T6-2	EN 1.4462	Transverse	755	847	4.77	52.39	250	489
T6-3	EN 1.4462	Transverse	755	847	4.90	50.68	248	479
T6-4	EN 1.4462	Transverse	755	847	4.82	50.42	243	478
T6-5	EN 1.4462	Transverse	755	847	4.80	50.57	243	468
T6-6	EN 1.4462	Transverse	755	847	4.72	47.14	222	436

Last, a study of Feber et al. presented in [8] and summarized in Table 4, focuses on the strength of longitudinal austenitic stainless steel fillet welds using the GTAW process. The study showed that for these specimens a β_w -factor of 0.9 would be possible.

Table 4: Overview of test results from Feber et al. [8]

Specimen	Grade	Load direction	Tensile strength base metal	Throat thickness	Throat length	Fracture surface	Ultimate strength
-	-	-	MPa	mm	mm	mm ²	kN
CS01	EN 1.4301	Longitudinal	599	3.06	48.21	148	248
CS02	EN 1.4301	Longitudinal	599	2.58	47.72	123	229
CS03	EN 1.4301	Longitudinal	599	3.12	47.86	149	248
CS05	EN 1.4301	Longitudinal	599	3.29	49.88	164	266
CS06	EN 1.4301	Longitudinal	599	3.13	49.14	154	256

4 Production of stainless steel fillet welds

4.1 Welding of stainless steel

The fact that stainless steel alloys exist with an austenitic, ferritic, martensitic or austenitic-ferritic (duplex) microstructure postulates the variety in behaviour of these alloys during welding. This behaviour is largely depending on the microstructure and composition of the alloy. In order to be able to predict the dominant microstructure for a given weld metal composition, Schaeffler [30] composed a diagram based on the chromium- and nickel-equivalent of stainless steels, measures for the amount of ferrite and austenite promoting elements respectively. The diagram distinguishes alloy compositions that lead to a certain microstructure. Bystram [31] linked specific regions in this diagram to the

occurrence of welding-related problems, caused by the heating and cooling imposed on the metal during welding, thus allowing to predict potential difficulties when welding a given alloy or alloy combination.

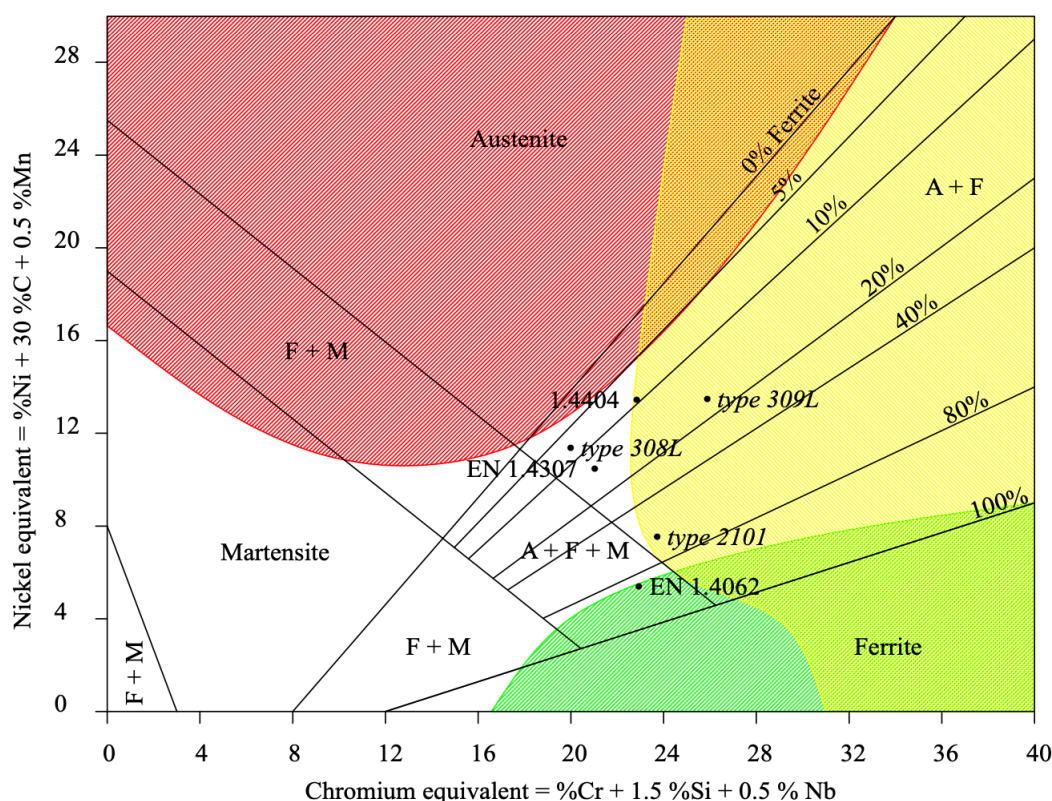


Fig. 2: Schaeffler diagram, where regions determined by Bystram [31] are annotated in red (hot cracking), yellow (sigma phase) and green (grain growth). Base materials and filler materials (cursive) used in this work are annotated on the graph as well.

Austenitic stainless steels are, as illustrated in Fig. 2, vulnerable to solidification cracking. High shrinkage strains in the weld pool, combined with the presence of low-melting phases, can cause a longitudinal fracture in the middle of the weld. The occurrence of solidification cracks in this type of microstructure can be attributed to the low solubility of the austenitic microstructure towards elements such as Sulphur and Phosphorus, often present in contaminants. The low solubility causes these elements to stay present in a liquid state, thus not being able to withstand the shrinkage strain and causing the weld metal to crack. In contrast, a ferritic microstructure allows for a higher solubility of these low-melting elements. Therefore, the presence of liquid phases at lower temperatures during solidification is prevented, avoiding the occurrence of solidification cracking.

Commercially available austenitic stainless steel alloys, such as the ones used in this study, EN 1.4307 and EN 1.4404, can contain a small amount of ferrite, as depicted in Fig. 3. However, the heating and

cooling cycle imposed during welding has an immense influence on the metallurgy of the weld metal. This results in differences between base metal and weld metal concerning mechanical properties, corrosion-resistance and the potential occurrence of solidification cracks.

In order to solve for the latter issues, a chemically overmatched filler material is selected that compensates for the detrimental effect of the thermal cycle imposed during welding. In the case of austenitic stainless steels, filler materials consist of an increased amount of ferrite. This ensures the absence of low-melting phases during solidification, as the elements out of which these consist are incorporated in the ferritic microstructure. Fig. 3 illustrates the difference in microstructure and ferrite content between the weld metal and the base metal.

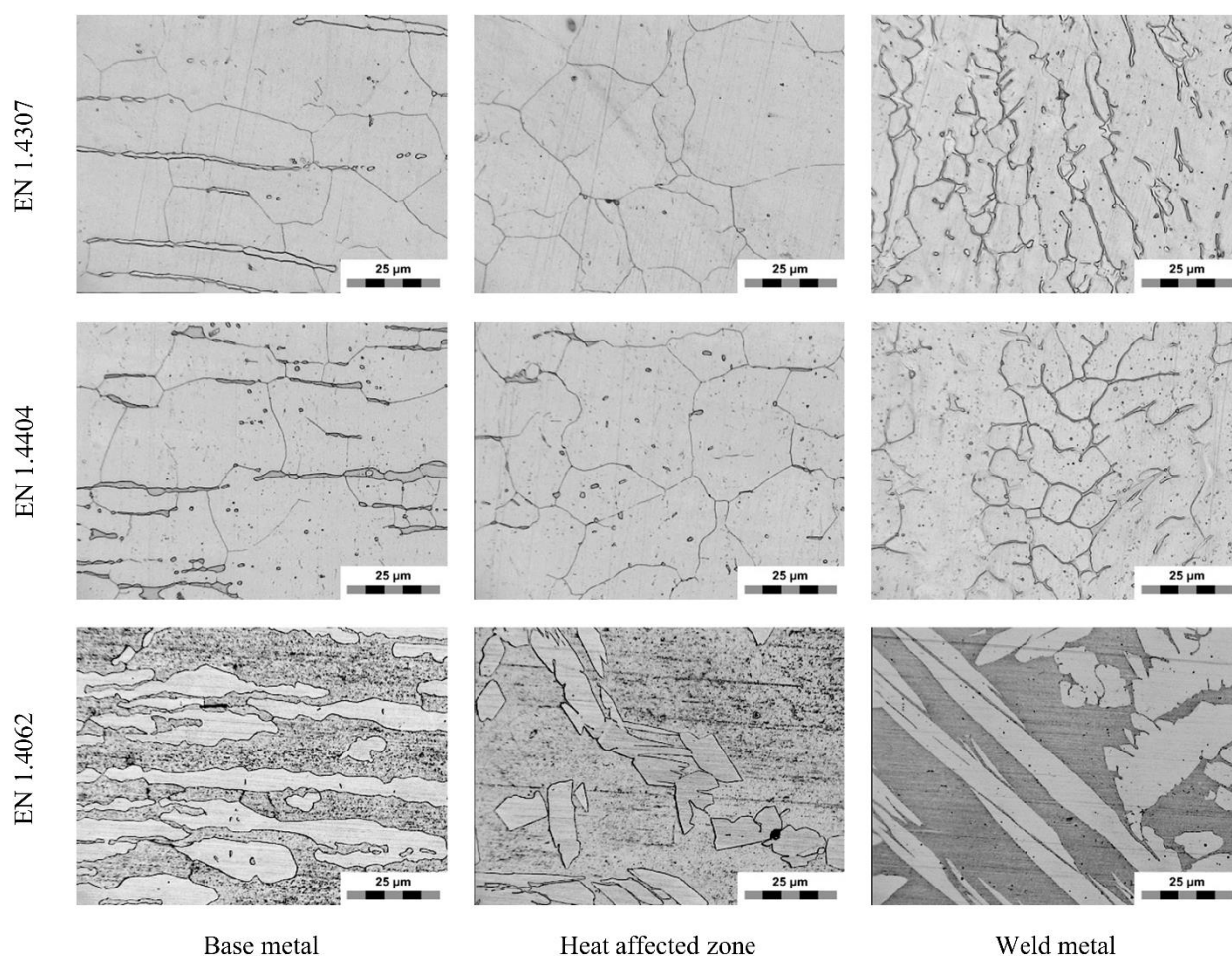


Fig. 3: Microstructure of (top) EN 1.4307, (middle) EN 1.4404 and (bottom) EN 1.4062 in (left) base metal, (centre) heat affected zone, (right) weld metal.

Duplex stainless steels are characterized by a microstructure where the base metal consists of both austenite and ferrite, approximately present in equal volumetric quantities. However, this phase balance can be heavily influenced by welding as rapid cooling, combined with ferritic solidification,

can prevent the formation of austenite and thus result in a relatively high ferrite content. A low amount of austenite will result in a lower toughness and ductility, while an excessive amount of austenite would affect the strength and the resistance to stress corrosion cracking in a negative way. In order to control the phase balance in the weld metal, duplex stainless steels are welded using a chemically overmatched filler metal by the addition of austenite-promoting elements, ensuring a sound phase balance despite the high cooling rates occurring in the weld metal. However, the heat affected zone in the base material is not affected by the overmatched filler material. Consequentially, the phase balance in this region can only be influenced by controlling the cooling rate, using a proper heat input – and thus process parameters – during welding.

Besides the austenite-ferrite balance, duplex stainless steels are prone to the formation of sigma phase. This intermetallic phase causes brittle behaviour of the material and could be formed during reheating above 580°C. For this reason, one must be careful performing heat treatments on duplex stainless steels. Apart from this, multi-layer welds can also cause the formation of sigma phase as the current pass heats up the previously welded layers. This can be prevented by using a maximum interpass temperature of 150°C.

4.2 Presently used welding conditions

In this study, alloys with an austenitic (EN 1.4307; EN 1.4404) and a duplex, austenitic-ferritic, (EN 1.4062) microstructure are welded by the GMAW and GTAW processes and tested in a destructive way. Although GTAW was included in this work, it should be noted that the productivity for this manual process is extremely low compared to other processes such as GMAW. Regarding the relevance towards construction engineering, it could thus be interesting to focus on welding processes with a higher efficiency such as GMAW and SAW or variants of these processes.

Table 5 lists the filler materials used for the base metals studied in this work. Although the welding filler materials often carry a trade name similar to the SAE/AISI-designation, they are typically chemically overmatched compared to the base metal. The austenitic filler materials contain an increased amount of Chromium to promote the presence of ferrite, whilst the lean-duplex filler material

contains an increased amount of Nickel to ensure a sound austenite-ferrite balance in the weld metal. It should be noted that in the case of EN 1.4307 base material, a type 308 filler material would be more generally applied, compared to the type 309 filler material used in this study. The latter finds more application in welding of dissimilar connections between carbon and stainless steels. However, due to a lack of availability, a type 309 was applied in this work. The use of this filler material is plausible in industrial situations, where both dissimilar (stainless steel to carbon steel) as well as similar stainless steel welds would be performed by the same welder.

EN 1.4307 and EN 1.4404 grades were both welded with an argon-based shielding gas, supplemented with 2,5 % CO₂. Arcal 129 gas, an argon-based shielding gas with additions of nitrogen, CO₂ and He, was used for the EN 1.4062 material. The heat input, also mentioned in Table 5, was calculated from the measured voltage, current and travel speeds, combined with the efficiency factor for the GMAW and GTAW process, 80% and 75% respectively [32]. This heat input, together with the workpiece geometry and interpass or preheat temperature, influences the heating and cooling rate and thus the metallurgy of the weld metal and heat affected zone.

Table 5: Welding parameters and filler materials used.

Base material	Process	Filler material ISO 14343-A	Filler material ISO 14343-B	Heat input kJ/mm
1.4307	GMAW	G 23 12 L Si	309 L Si	0.92
1.4404	GMAW	G 19 12 3 L Si	316 L Si	0.89
1.4062	GMAW	G 23 7 N L	2101	0.69
1.4062	GTAW	W 23 7 N L	2304	1.22

4.3 Quality assessment

Pre-production test pieces were subjected to visual inspection and the occurring imperfections were compared to the quality levels as mentioned in EN ISO 5817 [33]. The imperfections of the test pieces fell within the limits of quality level B, except intermittent undercut, which locally was inferior to quality level D.

The pre-production test pieces were cut, polished and etched for microstructural investigation. Test pieces of EN 1.4307 and EN 1.4404 were electrolytically etched in a 65% nitric acid solution at 3V during 80s, while EN 1.4062 was chemically etched with a Lichtenegger and Bloech solution. Their

respective microstructures can be found in Fig. 3. The austenite-ferrite balance plays an important role in the corrosion-related and mechanical characteristics of EN 1.4062 welds, and thus in their strength. This phase balance was calculated based on a grid counting method using microscopic images taken with a Hirox KH-8700 digital optical microscope at a magnification of 800x. The results of these tests are summarized in Table 6, together with the recommended values reported in [3]. The measured zones lie in between, or close to, the limits of the recommended values.

Both the used welding process and the welding parameters can influence the dilution of the base material in the weld metal. As a consequence of this phenomenon, the metallurgy – and thus the properties – of the weld metal gets influenced and diverges from the filler material composition. By taking the dilution into account when relating the strength of the weld to the base metal strength or weld metal strength, possibly more consistent relationships could be achieved. The dilution of the various welding conditions used in the experimental program are listed in Table 7.

On the same test pieces, Vickers hardness tests were performed in accordance with EN ISO 9015-1 [34]. By checking the location of the hardness measurements on the microscope, they could be divided between base material and weld metal. Measurements in the heat affected zone were not taken into account as this zone was too small in comparison with the width of the indentations of the hardness measurements. Although the differences in hardness between the weld metal and base material may be statistically relevant in some cases, the values lie very close to each other and no excessive differences in strength are expected.

Table 6: Ferrite content (%) of EN 1.4062 stainless steel welds in different regions.

	GMAW	GTAW	Recommended
Base metal	47	52	40 – 55
Heat affected zone	59	65	< 70
Weld metal	42	46	25 – 60

Table 7: Average hardness (HV5) and dilution (%) values for welded samples.

	1.4307 GMAW	1.4404 GMAW	1.4062 GMAW	1.4062 GTAW
Base metal	194	178	248	238
Weld metal	177	186	237	235
Dilution	39%	45%	38%	24%

As discussed above, generalising the mechanisms of strength of stainless steel welds could be inappropriate as different alloy groups, varying in microstructure, exist. Moreover, many stainless steel alloys are vulnerable to welding-related problems, so that their filler materials differ in chemical composition from the base material and the welding parameters are selected in ranges that omit the occurrence of these problems, depending on the welding process and workpiece geometry. As a result, the strength of the weldment could be dependent on the filler material, in combination with base material and its dilution, the welding process as well as the welding procedure.

5 Experimental program

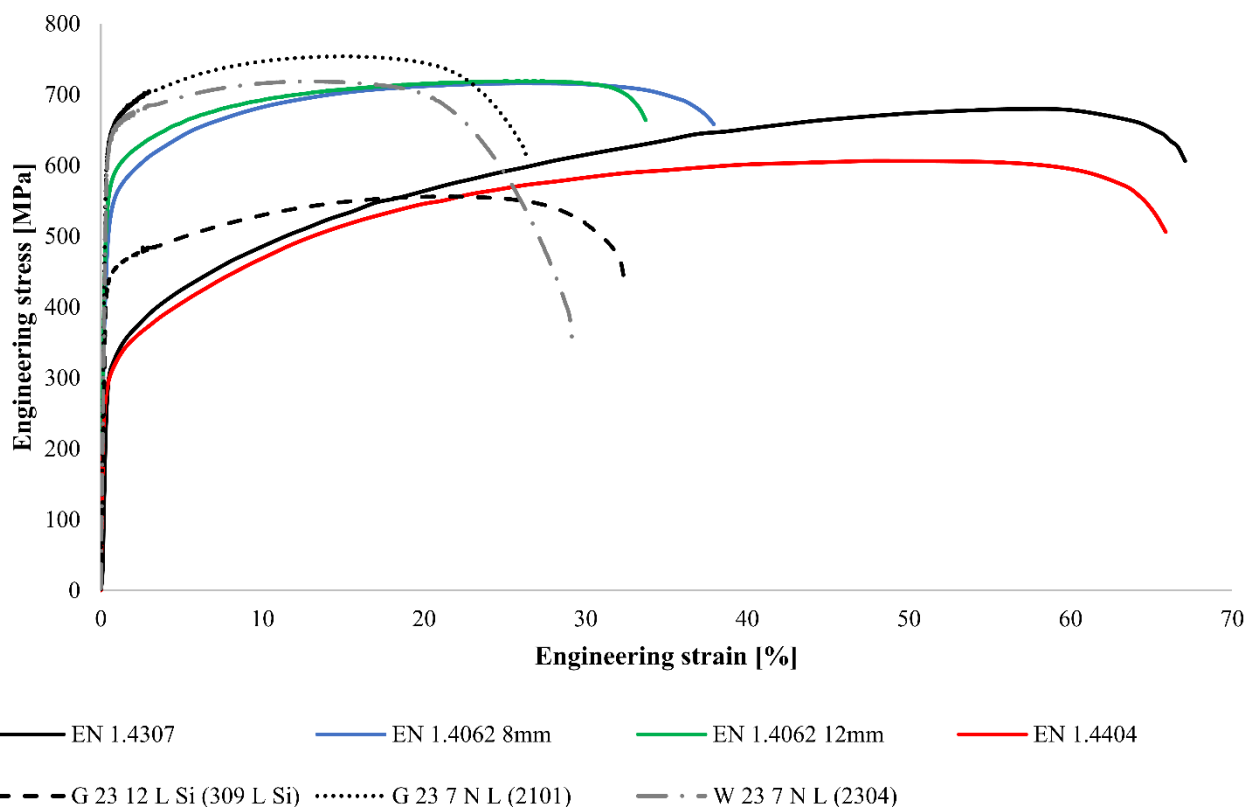
5.1 Mechanical properties of the base and weld metal

One of the essential parameters in the current design rules is the strength of the weakest joined part. Because no dissimilar joints were used, the ultimate strength of the base material should be used. For the three stainless steel grades, three coupons cut in the same direction as the welded specimens were tested. The two austenitic grades EN 1.4307 and EN 1.4404 exhibit a large ductility domain and significant strain hardening compared to the duplex grade EN 1.4062, which has a considerably higher yield strength combined with a smaller but still considerable ductility and strain hardening domain, as illustrated in Fig. 4.

The strength of the weld metal was tested according to EN ISO 5178 [35] and EN ISO 6892-1 [36] on an Instron 250kN tensile bench. The all-weld metal test specimens were fabricated according to type 1.3 of EN ISO 15792-1 [37] for three consumables welded with the corresponding process: G 23 12 L Si (309 L Si GMAW), G 23 7 N L (2101 GMAW) and W 23 7 N L (2304 GTAW). Due to a shortage, no tests were performed on the G 19 12 3 L Si (316 L GMAW) consumable. In Fig. 4, the consumables clearly show a higher yield strength than their corresponding base metal, but a reduced ductility. The dimensions of the test pieces, determined according to EN ISO 6892-1 [36], are presented in Table 8 together with the other details regarding material testing for base plate and weld metal.

Table 8: Mechanical properties of the coupons used for material testing of the base plate and weld metal.

Specimen	Process	b ₀ mm	t ₀ mm	d ₀ mm	L ₀ mm	f _y MPa	f _u MPa
1.4307	-	40.2	8.5	-	100	290	678
1.4404	-	40.3	8.1	-	100	270	609
1.4062 (8mm)	-	40.6	8.3	-	100	475	711
1.4062 (12 mm)	-	20.7	12.8	-	100	525	695
G 23 12 L Si (309 L Si)	GMAW	-	-	10.0	50	417	559
G 23 7 N L (2101)	GMAW	-	-	10.0	50	630	755
W 23 7 N L (2304)	GTAW	-	-	10.0	50	624	719

**Fig. 4: Engineering stress strain curve for base material and all-weld metal.**

5.2 Experimental results

The experimental study focuses on the strength of fillet welds welded using GMAW or GTAW in two loading directions and three stainless steel grades: two austenitic grades EN 1.4307 (304L) and EN 1.4404 (316L), and one duplex grade EN 1.4062. Half of the tests were carried out with the load perpendicular to the welds causing both normal σ_{\perp} (perpendicular to the weld plane) and shear stresses τ_{\perp} (perpendicular to the weld throat axis), which are denominated in this paper and in literature as transverse loaded welds. The other half of the tests with the load parallel to the weld causing only shear stresses $\tau_{//}$ (parallel to the weld throat axis), are denominated as longitudinally loaded welds. An overview of the specimens and used dimensions is presented in Fig. 5 and Table 9.

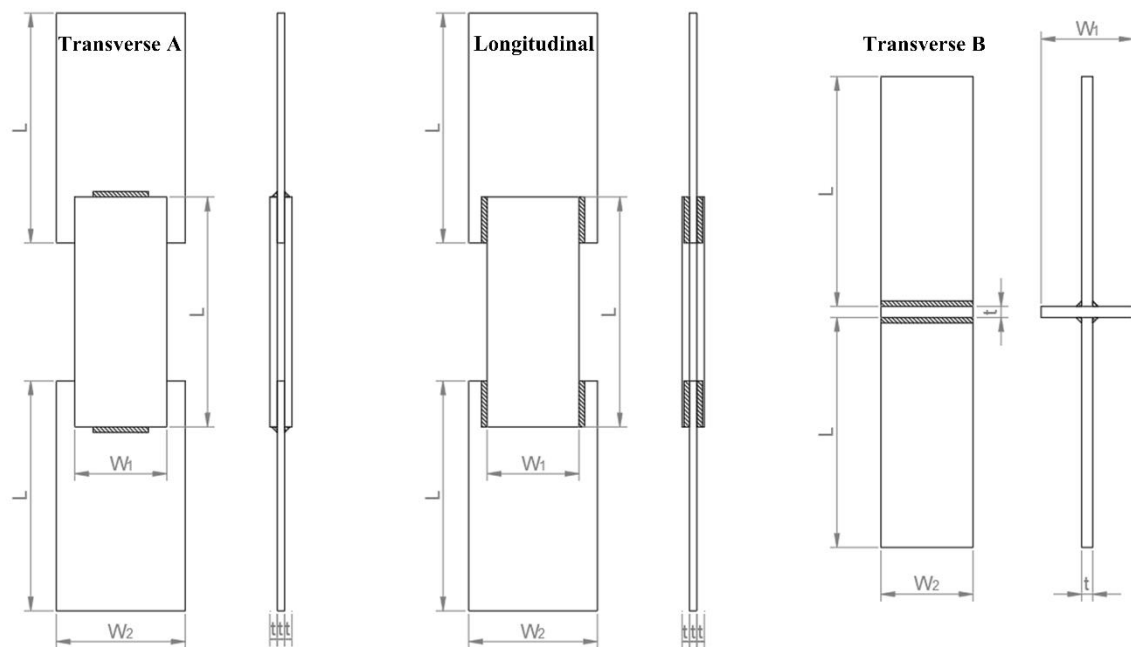


Fig. 5: Overall dimensions of the specimens – perpendicular (up) or parallel (down) to the loading direction.

Table 9: Overview of the dimensions of the tested specimens.

Specimen	Process	Direction	Amount	a_{nom} mm	L_{nom} mm	t mm	L mm	W_1 mm	W_2 mm
1.4307L1-3	GMAW	Longitudinal	3	4	40	8	250	100	140
1.4307T1-3	GMAW	Transverse A	3	4	60	8	250	100	140
1.4404L1-3	GMAW	Longitudinal	3	4	40	8	250	100	140
1.4404T1-3	GMAW	Transverse A	3	4	60	8	250	100	140
1.4062L1-3	GMAW	Longitudinal	3	4	50	8	250	100	140
1.4062T1-3	GMAW	Transverse A	3	4	75	8	250	100	140
1.4062L4-6	GTAW	Longitudinal	3	3	50	12	250	60	100
1.4062T4-6	GTAW	Transverse B	3	3	100	12	250	100	100

Two hydraulic tensile testing benches were used to perform the experimental program: a Wolpert 1000kN tensile bench and an Instron HDX1500kN tension and compression bench. The load was applied quasi statically with an average speed lower than 0.01 mm/s. The initial geometry of the weld was measured using stereovision digital image correlation (DIC) and compared to the fracture surface after the test. Stereovision DIC is an optical measurement system that uses pictures taken by synchronized cameras of a speckle pattern on the specimens in the undeformed and deformed state. More information on this method can be found in [38] or more elaborate in [39]. During the tests, some welds were measured optically using DIC, visualized in Fig. 6. This system allows us to follow the displacement field of both plates and of the weld, before cracking. Strain fields in and around the weld are calculated based on the displacement field, which allows to localize the crack initiation based on strain concentrations, as presented in Fig. 6 for a transverse loaded weld. Furthermore, a load-displacement curve of the weld is determined by comparing the displacements of the plates just above and just under the weld, as presented in Fig. 7 for the GMAW specimens.

As can be seen in Fig. 7, all failure modes are ductile. All cracks initiate in the start or end zone of the weld (in the end crater for most welds) and propagate until failure is reached. Typical failure modes can be seen in Fig. 8 for a longitudinal and a transverse weld. Because the failure occurs in the weld metal, it can be concluded that the undercut, which is visible in some welds, does not have an influence on the ultimate loads. By measuring the weld throat over the whole length of the weld, the reduced area in the end zone can be considered in the evaluation of the strength. An overview of the results of the experimental program is presented in Table 10.

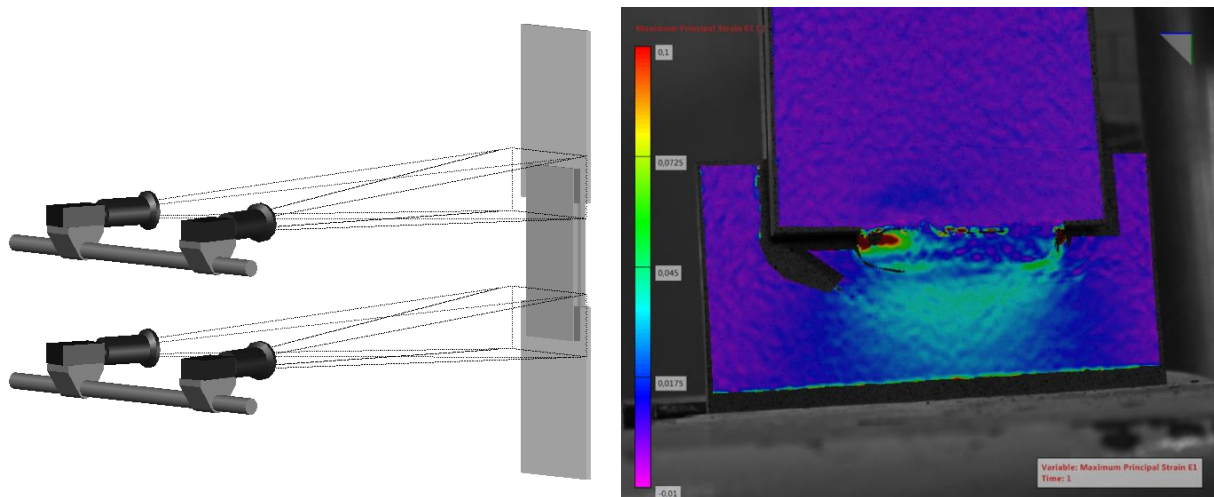


Fig. 6: Measurement set-up to measure displacements and strains using DIC (left) and measured strain pattern for a transverse weld (right).

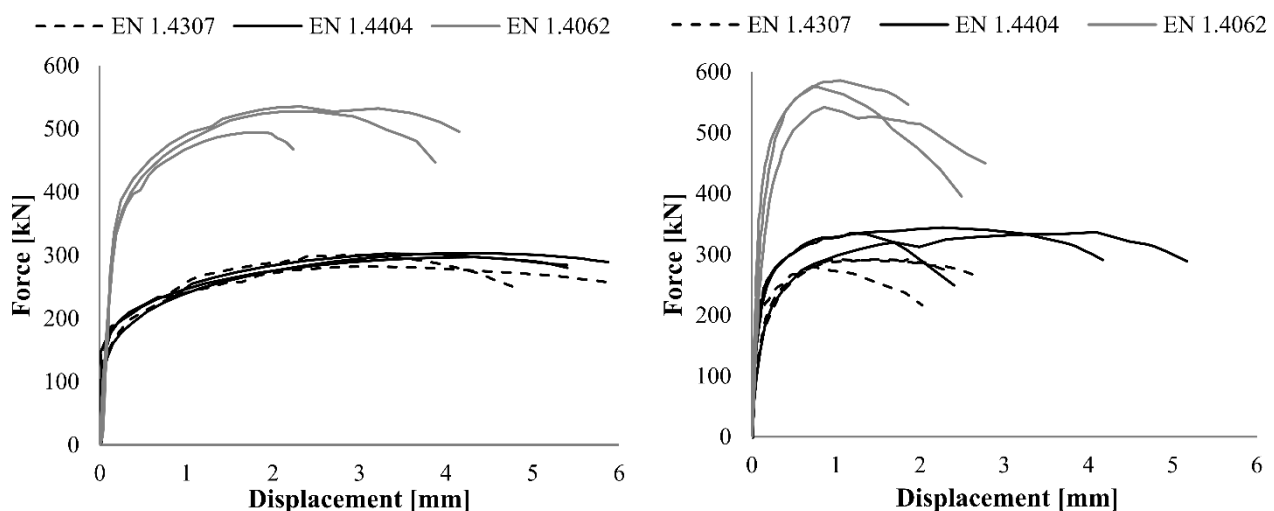


Fig. 7: Force-displacement curves of longitudinal welds (left) and transverse welds (right).



Fig. 8: Typical failure mode for longitudinal welds (left) and transverse welds (right).

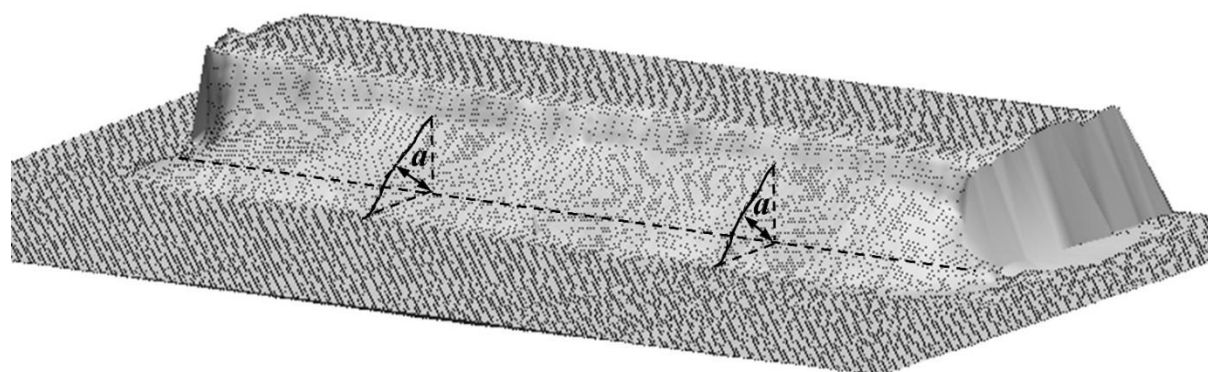
5.3 Measurement of the weld surface

The area of the weld throat plane has a direct influence on the ultimate strength of the weld. Herein, multiple methods were used to evaluate this surface. The weld throat surface can be calculated using the nominal design values and the design rules in EN 1993-1-8 [9], as explained in section 2. However, in reality, the effective weld throat is larger than that. Moreover, in the start and end zone, a divergence to this ideal value was noticed. It is therefore important to measure the weld throat surface over the whole length of the weld, which was presently done using DIC. Two methods are used: one before testing and one after failure.

Before testing, static pictures of the weld are taken with MatchID [40], the software used for taking and post-processing the DIC pictures, and a cloud of points of the outer surface of the weld is generated as can be seen in Fig. 9. A post processing software, in this case Cloudcompare [41], was used to calculate the actual throat thickness. The intersection of the surface of the bottom plate and of the side surface of the top plate was determined. From this line, the throat thickness a is measured at a 45° angle, which is theoretically the critical plane. Multiple angles were measured, confirming that the 45° angle corresponds well with the minimal area.

Table 10: Overview of experimental results.

Specimen	Grade	Welding process	Load direction	Tensile strength base metal	Tensile strength weld metal	Fracture surface	Ultimate strength	Fracture angle
-	-	-	-	MPa	MPa	mm ²	kN	°
4307L1	EN 1.4307	GMAW	Longitudinal	678	559	192	302	25
4307L2	EN 1.4307	GMAW	Longitudinal	678	559	188	299	51
4307L3	EN 1.4307	GMAW	Longitudinal	678	559	177	284	32
4307T1	EN 1.4307	GMAW	Transverse	678	559	258	297	45
4307T2	EN 1.4307	GMAW	Transverse	678	559	250	281	45
4307T3	EN 1.4307	GMAW	Transverse	678	559	250	292	42
4404L1	EN 1.4404	GMAW	Longitudinal	609	/	182	303	66
4404L2	EN 1.4404	GMAW	Longitudinal	609	/	183	297	54
4404L3	EN 1.4404	GMAW	Longitudinal	609	/	189	303	55
4404T1	EN 1.4404	GMAW	Transverse	609	/	290	338	47
4404T2	EN 1.4404	GMAW	Transverse	609	/	281	337	43
4404T3	EN 1.4404	GMAW	Transverse	609	/	306	343	44
4062L1	EN 1.4062	GMAW	Longitudinal	711	755	268	529	49
4062L2	EN 1.4062	GMAW	Longitudinal	711	755	250	495	41
4062L3	EN 1.4062	GMAW	Longitudinal	711	755	275	536	49
4062T1	EN 1.4062	GMAW	Transverse	711	755	479	576	24
4062T2	EN 1.4062	GMAW	Transverse	711	755	457	587	34
4062T3	EN 1.4062	GMAW	Transverse	711	755	417	543	29
4062L4	EN 1.4062	GTAW	Longitudinal	695	719	129	285	45
4062L5	EN 1.4062	GTAW	Longitudinal	695	719	147	301	51
4062L6	EN 1.4062	GTAW	Longitudinal	695	719	146	297	42
4062T4	EN 1.4062	GTAW	Transverse	695	719	288	384	34
4062T5	EN 1.4062	GTAW	Transverse	695	719	282	381	39
4062T6	EN 1.4062	GTAW	Transverse	695	719	263	353	34

**Fig. 9: 3D point cloud of a measured weld with DIC.**

As EN 1993-1-8 [9] mentions, a deep penetration of the weld in the base material significantly increases the strength of the weld. In the macroscopic investigation, a large penetration was noticed up to 2.5mm for the EN 1.4404 specimens. The measured throat thickness was hence enlarged along the effective length of the weld, i.e. along $l - 2a$ as described in Section 2 (in the start and end zones, lower penetration occurs). This surface is called A_{eff} , as in equation 3 where i is the penetration which was measured in the macroscopic examination for every grade.

$$A_{eff} = a_{eff} * l_{eff} + i * (l_{eff} - 2a_{eff}) \quad (3)$$

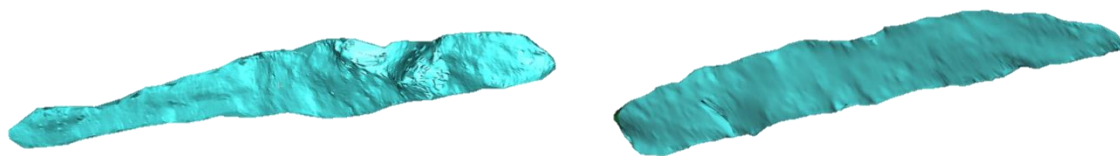
1 where: A_i is the area used in equation 1 and 2 to determine the stresses for method i

2 a_{eff} is the effective throat thickness measured using DIC

3 l_{eff} is the effective length of the weld measured using DIC

4 i is the extra penetration measured using the macroscopic investigation.

5 The other method to assess the weld area is to measure the fracture area after the tests. The roughness
6 of the fracture surface and the varying fracture angle along the weld length have to be taken into
7 account. Analog to the measurements of the effective throat thickness, the fracture areas of all the
8 specimens were measured using DIC. The resulting point cloud of this surface was generated using
9 MatchID [40]. Afterwards, CloudCompare [41] was used to calculate the area of the meshed cloud of
10 points. Fig. 10 provides two different images of two fracture surfaces after post-processing the DIC
11 images with Cloudcompare [41]. In Table 11, the measured fracture surfaces are also provided. It is,
12 on average, 10 % lower than the one obtained by the previous method i.e. equation 3. The penetration,
13 which is not constant over the length of the weld due to manual welding, and the local imperfections
14 in the weld explain this difference. Both methods are compared here below for all tests using GMAW.
15 A relatively high difference is observed and can reach, on average, 20% of relative difference leading
16 to a proportional influence on the calculated failure load.



17
18 **Fig. 10: Post-process images of fracture surfaces using DIC and Cloudcompare.**
19

Table 11: Nominal dimensions of welds according to equation (3) and fracture surface [mm²]

Name	Load Direction	Measured Fracture Surface	Measured A_{eff} (equation 3)	Relative difference %
1.4307L1	Longitudinal	192	182	5
1.4307L2	Longitudinal	188	197	5
1.4307L3	Longitudinal	177	193	9
1.4307T1	Transverse	258	335	30
1.4307T2	Transverse	250	309	24
1.4307T3	Transverse	250	315	26
1.4404L1	Longitudinal	182	223	23
1.4404L2	Longitudinal	183	210	14
1.4404L3	Longitudinal	189	222	18
1.4404T1	Transverse	290	401	38
1.4404T2	Transverse	281	417	49
1.4404T3	Transverse	306	433	42
1.4062L1	Longitudinal	268	307	15
1.4062L2	Longitudinal	250	291	16
1.4062L3	Longitudinal	275	307	12
1.4062T1	Transverse	479	567	18
1.4062T2	Transverse	457	559	22
1.4062T3	Transverse	417	503	21

6 Assessment of the design rules and reliability

The design rules for stainless steel fillet welds are assessed based on the 24 experiments presented in this paper in combination with the 70 experiments listed in section 3. These tests include 48 tests on longitudinal welds and 46 tests on transverse welds. Furthermore, in these tests, three different welding processes are included: 69% of the tests were performed on GTAW welded specimens, 19% on GMAW, and 12% on specimens welded with SMAW. To assess the design strength for these specimens, the experimental failure load is compared to the predicted failure load using the design rules in EN 1993-1-8 [9]. For the comparison, the safety factor γ_{M2} and the correlation factor β_w are set equal to 1. In Fig. 11, the experimental failure load is presented compared to the predicted strength. Except for some tests in [5], all experimental-to-predicted strength ratios are on the safe side. However, the majority of experiments have a considerable overstrength with a majority of experimental-to-predicted strength ratios higher than 1.20. An overview of the average strength ratios and standard deviations per reference, grade and welding process is given in Table 12. The overall average per stainless steel family clearly shows a high scatter on the results, while the scatter per reference and grade is relatively small.

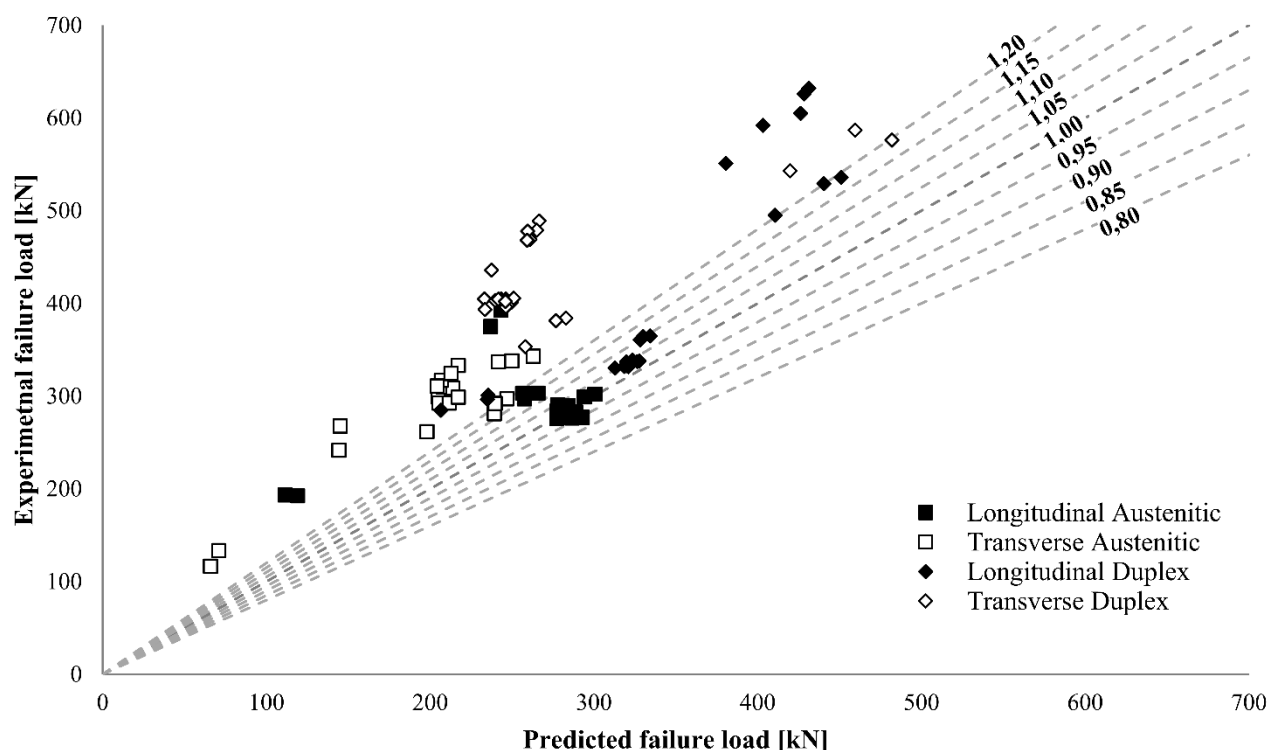


Fig. 11: Overview of the experimental and predicted failure loads for all experiments on stainless steel fillet welds.

Table 12: Overview of the strength ratios for all tests.

Reference	Welding process	Grade	Longitudinal		Transverse	
			Strength ratio	Standard deviation	Strength ratio	Standard deviation
	Austenitic		1.16	0.23	1.47	0.19
Tests	GMAW	EN 1.4307	1.01	0.01	1.20	0.02
Tests	GMAW	EN 1.4404	1.16	0.02	1.35	0.04
Stangenberg [5]	GTAW	EN 1.4301	1.00	0.03	1.45	0.07
Lee et al. [6]	GTAW	EN 1.4301	1.64	0.07	1.79	0.09
Feber et al. [8]	GTAW	EN 1.4301	1.23	0.07		
	Duplex		1.20	0.17	1.61	0.19
Tests	GMAW	EN 1.4062	1.20	0.01	1.26	0.05
Tests	GTAW	EN 1.4062	1.31	0.06	1.37	0.01
Stangenberg [5]	GTAW	EN 1.4462	1.06	0.03	1.66	0.04
Yang et al. [7]	SMAW	EN 1.4462	1.46	0.03	1.82	0.02

In the experiments performed in this paper, a clear variation is visible between the two austenitic grades with an average ratio of 1.01 for EN 1.4307 and 1.16 for EN 1.4404. However, the low strength ratio of EN 1.4307 is caused by the relatively low tensile strength of the used filler material with a tensile strength of 559 MPa only compared to the high ultimate strength of the base material which reaches 678 MPa. In [5], the low strength ratios also have a lower tensile strength in the weld metal than in the base metal. However with respectively 617 MPa and 659 MPa, the difference is less severe. Important to note is that, in both cases, the strength of the weld metal is still considerably higher than the nominal tensile strength of the base material, which would ensure a safe design. Since all failure modes occur in the weld metal, the all-weld metal ultimate strength leads to a more reasonable comparison when

calculating the strength of the connection. By using the ultimate strength of the weld metal in equation 2, the average strength ratio of the austenitic specimens increases, as can be seen in Table 13, considering that all austenitic all-weld specimens had a lower ultimate strength than their corresponding base metal. For the duplex stainless steel grades, the strength ratios decrease since the weld metal is in all references stronger than the corresponding base metal.

Table 13: Overview of the strength ratios for all tests when utilizing ultimate strength of all-weld metal.

Reference	welding process	Grade	Longitudinal		Transverse	
			Strength ratio	Standard deviation	Strength ratio	Standard deviation
	Austenitic		1.29	0.38	1.67	0.28
Tests	GMAW	EN 1.4307	1.23	0.01	1.45	0.03
Stangenberg [5]	GTAW	EN 1.4301	1.06	0.03	1.55	0.07
Lee et al. [6]	GTAW	EN 1.4301	1.98	0.08	2.16	0.11
	Duplex		1.24	0.08	1.44	0.20
Tests	GMAW	EN 1.4062	1.13	0.01	1.18	0.05
Tests	GTAW	EN 1.4062	1.26	0.06	1.32	0.01
Yang et al. [7]	SMAW	EN 1.4462	1.29	0.02	1.62	0.02

The following reliability analysis was made following the methodology proposed in EN 1990:2002 annex D [42]. In [43], the proposed coefficients of variation for f_u , based on statistical data on material and geometric parameters from stainless steel producers, for austenitic, ferritic and duplex grades is 0.035. The coefficient of variation of the geometric properties is considered equal to 0.05, which was also utilized for stainless steel in the development of the AISC stainless steel design guide [44]. In the present analysis, the scatter of the (r_{ti} , r_{ei}) values was too high to give economical design resistance functions. Therefore, the total test population was divided into appropriate sub-sets depending on the considered grade. The Clause D.8.2.2.5 of EN 1990 Annex D [42] was used, which allows the use of the total number of tests in the original series for determining the $k_{d,n}$ fractile factor to avoid large safety factors due to a low amount of data points in each sub-set. Analogous to the reliability analysis by Afshan et al. in [43], an over-strength factor for f_u equal to 1.1 was taken into account. A similar over-strength factor could be used for the geometry of the weld since the specified throat height is the minimal throat height over the length of the weld rounded down to the mm and therefore the mean throat plane will always be bigger than the nominal one. However, no sufficient statistical data is available to take this factor into account.

The results of this analysis are presented in Table 14, where n is the total number of data points for tests (note that n is always lower than 100), and b is the average experimental-to-model resistance ratio based on a least squares fit of the slope of the r_{ei} versus r_{ti} plot for each set of data. The coefficient of variation V_δ of the error term $\delta_i = r_{ei}/b r_{ti}$ is used as a measure of the variabilities of the predictions obtained from the resistance function, γ_{M2} is the partial safety factor for the failure resistance of welds, and β_w is the correlation factor corresponding to the normative partial safety factor γ_{M2} equal to 1.25.

Table 14: Overview of the reliability analysis.

Subset	n	b	V_δ	γ_{M2}	β_w
All specimens	94	1.299	0.231	1.49	1.19
Longitudinal	48	1.171	0.168	1.36	1.09
Longitudinal duplex	22	1.226	0.139	1.20	0.96
Tests	6	1.220	0.056	0.96	0.77
Stangenberg [5]	11	1.057	0.025	1.05	0.84
Yang et al. [7]	5	1.462	0.018	0.76	0.61
Longitudinal austenitic	26	1.085	0.189	1.57	1.26
Tests	6	1.077	0.073	1.14	0.91
Stangenberg [5]	11	0.977	0.033	1.15	0.92
Lee et al. [6]	4	1.613	0.040	0.71	0.57
Feber et al. [8]	5	1.216	0.053	0.96	0.77
Transverse	46	1.501	0.181	1.10	0.88
Transverse duplex	24	1.551	0.200	1.13	0.90
Tests	6	1.282	0.055	0.91	0.73
Stangenberg [5]	12	1.612	0.022	0.69	0.55
Yang et al. [7]	6	2.230	0.050	0.52	0.42
Transverse austenitic	22	1.401	0.133	1.03	0.82
Tests	6	1.276	0.069	0.95	0.76
Stangenberg [5]	12	1.453	0.048	0.80	0.64
Lee et al. [6]	4	1.773	0.051	0.66	0.53

It can be seen from Table 14 and Table 15 (as well as from Fig. 11) that a division into subsets based on loading direction and stainless steel family is reasonable since the correction factor b clearly differs in between subsets. Moreover, the longitudinal loading direction is the most critical direction in the design of fillet welds, which was also mentioned by numerous authors in the literature [5], [18], [19].

Table 15: Overview of the reliability analysis when utilizing ultimate strength of all-weld metal.

Subset	n	b	V_{δ}	γ_{M2}	β_w
All specimens	60	1.299	0.217	1.49	1.19
Longitudinal	29	1.213	0.207	1.54	1.23
Longitudinal duplex	11	1.235	0.065	0.98	0.78
Tests	6	1.155	0.068	1.06	0.85
Yang et al. [7]	5	1.295	0.014	0.85	0.68
Longitudinal austenitic	18	1.173	0.263	1.91	1.53
Tests	3	1.230	0.009	0.89	0.71
Stangenberg [5]	11	1.064	0.029	1.05	0.84
Lee et al. [6]	4	1.947	0.040	0.59	0.47
Transverse	31	1.421	0.165	1.14	0.91
Transverse duplex	12	1.358	0.144	1.12	0.90
Tests	6	1.215	0.068	1.00	0.80
Yang et al. [7]	6	1.622	0.011	0.68	0.54
Transverse austenitic	19	1.568	0.162	1.03	0.82
Tests	3	1.454	0.019	0.76	0.61
Stangenberg [5]	12	1.555	0.049	0.75	0.60
Lee et al. [6]	4	2.140	0.051	0.55	0.44

However, within these subsets the correction factor b remains inconsistent, resulting in high (to sometimes very high) coefficients of variation V_{δ} . Extra subsets proposing a division per reference show safety factors ranging from 0.76 to 1.05 for duplex specimens loaded in the longitudinal direction compared to 1.20 for the whole subset, while for austenitic stainless steel specimens in the longitudinal direction the safety factor ranges from 0.71 to 1.15 for the individual subsets with an overall safety factor of 1.57 for the whole subset, leading to unreasonable β_w factors.

Multiple reasons could be the cause of the high scatter between the references. Firstly, different welding procedures were used by the authors and, as shown in section 4 of this paper, the welding procedure and corresponding microstructure can influence the strength of the weld. Since different welding procedures and filler materials are also used in practise, it would be unwise to disregard this effect by determining the safety factor based on the individual subsets. However, when the all-weld ultimate strength of the filler material is taken into account, as shown in Table 15, the scatter between the references is still visible which leads to the conclusion that, although the welding procedure and choice of filler material plays a role in the strength of the fillet weld, it is not the main cause of the high variability observed between the references.

Secondly, various measurement techniques were used by the authors and, as shown in paragraph 5.3, this could have a major impact on the predicted failure load. Since this variation is accounted for in

the references but is not applicable in industry where minimum throat heights and lengths are specified, the safety factor of the individual subsets could safely be used in practise.

7 Recommendations and future works

Further investigations should be made to better understand the variation between the available references. To minimize the scatter between multiple references, we recommend that a more standardized method should be used to examine the strength of fillet welds. The method should include all information concerning the welding procedure and should include the measurement method used to determine the area of the critical plane. This would lead to more consistent experimental results and more coherent correlation factor for stainless steel fillet welds.

Moreover, more experimental data to examine the influence of the welding procedure, including welding process, filler materials, heat input and the corresponding microstructure for stainless steel, is needed. Currently, 69% of the experimental data consists of specimens welded using GTAW, while this process is rarely used in civil engineering, and no results are available for more commonly used processes, such as SAW. Furthermore, more data is needed to adequately take into account complex loading conditions. Considerable conservatism is currently present for transverse welds and only limited information is available on the strength of inclined stainless steel fillet welds. Additionally, Lee et al. [6] noticed that a superposition of the resistances when combining longitudinal and transverse welds is not sufficient for the prediction of the failure load.

8 Conclusions

In this paper, the applicability of the design rules in EN 1993-1-8 [9] and EN 1993-1-4 [10] is assessed based on 94 experiments on stainless steel welded specimens. The experimental programme includes 24 experiments made of 3 stainless steel grades: austenitic EN 1.4307, also known as 304L, austenitic EN 1.4404, or 316L, and lean duplex EN 1.4062. Three welding processes are included: GTAW (TIG), GMAW (MAG) and SMAW (MMA). Two loading directions were considered. The following conclusions are drawn:

- The transverse loading direction, causing a combination of normal (perpendicular to the weld throat plane) and shear (in the weld throat plane, perpendicular to the weld throat axis) stresses, clearly showed a higher experimental-to-predicted strength ratio for all grades. The longitudinally loaded specimens, causing shear stresses (in the weld throat plane, parallel to the weld throat axis), showed a lower strength ratio.
- Based on these test results and the ones collected from the literature, it could be concluded that the current European design rules [9]-[10], using a β_w of 1.0, give conservative predictions for all grades and loading directions. The average experimental-to-predicted strength ratios for duplex stainless steel specimen suggests that a lower correlation factor β_w for these grades should be recommended.
- The reliability analysis showed that the design rules for stainless steel fillet welds should be divided into subsets for the loading direction and stainless steel family. The safety factor γ_{M2} and correlation factor β_w are controlled by the longitudinal strength of welds. The duplex stainless steel welds have a slightly better performance than the austenitic family. However, the scatter within these subsets remained high which lead to high safety factors. Further dividing these subsets by reference leads to acceptable coefficients of variation. Since the use of the all-weld metal strength had a minor influence on the scatter within the subset, the main influence is the measurement method of the throat plane, taking correctly into account the variation on the throat height and the penetration in the base metal along the length of the weld. The most critical individual correlation factor per family for longitudinal welds would lead to a correlation factor of 0.84 for duplex stainless steel welds and 0.92 for austenitic stainless steel fillet welds.

9 Acknowledgements

The first author is funded by a PhD fellowship from the Research Foundation Flanders. We would also like to thank Industeel for providing the duplex material for this research.

References

- [1] International stainless steel forum, Stainless steel in architectural applications, 2016
- [2] Baddoo, N.R., Kosmač, A. Sustainable Duplex Stainless Steel Bridges, (www.wordstainless.org). 2010
- [3] Van Nassau, L., Meelker, H., Hilkes, J. Welding duplex and super-duplex stainless steels, a guide for industry. *Welding in the world*, 31 (5), 322-343, 1993
- [4] Kotecki, D.J. Some Pitfalls in Welding of Duplex Stainless Steels. *Soldagem & Inspeção*, 15 (4), 336-343, 2010.
- [5] Stangenberg, H. Final report. ECSC Project – Development of the use of stainless steel in construction, tech. Rep. RT810, contract No. 7210 SA/842. The steel construction institute, 2000.
- [6] Lee, H., Hwang, B., Kim, T. Ultimate strength of austenitic stainless steel fillet-welded connections with weld metal fracture. *Thin-Walled Structures*, 116, 145-153, 2017.
- [7] L. Yang, X. Wei, M. Li, and Y. Zhang, Strength of Duplex Stainless Steel Fillet Welded Connections. *Journal of Constructional Steel Research*, 152, 246-260, 2019.
- [8] Feber, N., Jandera, M., Forejtova, L., Kolarik, L. Stainless steel fillet weld tests. *Proceedings of the international colloquium on stability and ductility of steel structures 2019*. Prague, Czech Republic, 2019.
- [9] European Committee for Standardization (CEN), Eurocode 3: design of steel structures - part 1-8: Design of joints. EN 1993-1-8:2005.
- [10] European Committee for Standardization (CEN), Eurocode 3: Design of steel structures - Part 1-4: General rules - Supplementary rules for stainless steels, EN 1993-1-4/A1:2015.
- [11] Kuhlmann, U., Günther, H.-P., Rasche, C. High-strength steel fillet welded connections. *Steel Construction*, 1, 77-84, 2008.
- [12] Fortan, M., Dejans, A., Debruyne, D., Rossi, B. The strength of stainless steel fillet welds using GMAW. *Proceedings of Stainless Steel in Structures: Fifth International Experts Seminar*. London, United Kingdom, 2017.
- [13] Fortan, M., Dejans, A., Debruyne, D., Rossi, B. Experimental study on the strength of stainless steel fillet welds. *Proceedings of the 18th International Conference on Experimental Mechanics*. Brussels, Belgium, 2018.
- [14] Günther, H.P., Hildebrand, J., Rasche, C., Versch, C., Wudtke, I., Kuhlmann, U., Vormwald, M., Werner, F. Welded connections of high-strength steels for the building industry. *Welding in the world*, 56, 86-106, 2012.
- [15] Collin, P., Johansson, B. Design of welds in high strength steel. *International conference on steel and composite structures*. Maastricht, The Netherlands, 2005.
- [16] Khurshid, M., Barsoum, Z., Mumtaz, N.A. Ultimate strength and failure modes for fillet welds in high strength steels. *Materials and Design*, 40, 36-42, 2012.
- [17] European Committee for Standardization (CEN), Eurocode 3: design of steel structures - part 1-12: Additional rules for the extension of EN 1993 up to steel grades S 700. EN 1993-1-12:2007.
- [18] Björk, T., Toivonen, J., Nykänen, T. Capacity of fillet welded joints made of ultra high strength steel. Finland: Lappeenranta University of Technology, 2012.
- [19] Lu, H., Dong, P., Boppudi, S. Strength analysis of fillet welds under longitudinal and transverse shear conditions. *Marine structures*, 43, 87-106, 2015.
- [20] Luo, J., Dong, Y., Li, L., Wang, X. Microstructure of 2205 duplex stainless steel joint in submerged arc welding by post heat treatment. *Journal of manufacturing process*, 16, 144-148, 2013.
- [21] Lakshminarayanan, A.K., Shanmugam, K., Balasubramanian, V. Effect of welding processes on tensile and impact properties, hardness and microstructure of AISI 409M ferritic stainless joints fabricated by duplex stainless steel filler metal. *Journal of iron and steel research, international* 16, 66-72, 2009.
- [22] Mohandas, T., Reddy, G.M., Naveed, M. A comparative evaluation of gas tungsten and shielded metal arc welds of a “ferritic” stainless steel. *Journal of materials processing technology*, 94, 133-140, 1998.

- [23] Asif, M.M., Shrikrishna, K.A., Sathiya, P., Goel, S. The impact of heat input on the strength, toughness, microhardness, microstructure and corrosion aspects of friction welded duplex stainless steel joints. *Journal of manufacturing processes*, 18, 92-106, 2014.
- [24] Rahmani, M., Eghlimi, A., Shamanian, M. Evaluation of microstructure and mechanical properties in dissimilar austenitic/super duplex stainless steel joint. *Journal of materials engineering and performance*, 23, 3745-3753, 2014.
- [25] Gotkowski, P., Jachym, R., Fryc, H. Duplex steel welding in the construction of railway vehicles. *Welding International*, 28 (12), 917-922, 2013.
- [26] Kumar, S., Shahi, A.S. Effect of heat input on the microstructure and mechanical properties of gas tungsten arc welded AISI 304 stainless steel joints. *Materials and design*, 32, 3617-3623, 2010.
- [27] Luo, J., Wang, X., Yao, Z. Double-sided single-pass submerged arc welding for 2205 duplex stainless steel. *Journal of materials engineering and performance*, 22 (9), 2477-2486, 2012.
- [28] Ohata, M., Namekata, T., Satoh, S., Okazaki, T., Shimura, Y., Watanabe, H. Load-carrying capacity of overmatched welded joint of stainless steel for building structure. *Weld world*, (28), 743-753, 2012.
- [29] Westin, E.M. Microstructure and properties of welds in the lean duplex stainless steel LDX 2101®. Doctoral thesis Royal Institute of Technology Stockholm, 2010.
- [30] Schaeffler A.L. Welding dissimilar metals with stainless electrodes. *Iron Age*, 162:72, 1948.
- [31] Bystram, M. C. T. Some aspects of stainless alloy metallurgy and their application to welding problems. *British Welding Journal*, 3.2, 41-46, 1956.
- [32] Stenbacka, N., Choquet, I., & Hurtig, K. (2012). Review of Arc Efficiency Values for Gas Tungsten Arc Welding. IIW Commission IV-XII-SG 212 Intermediate Meeting BAM , Berlin , Germany 18-20 April , 2012 Doc . XII-2070-12 / 212-1229-12.
- [33] EN ISO 5817. Welding - Fusion-welded joints in steel, nickel, titanium and their alloys (beam welding excluded) - Quality levels for imperfections. International Organization for Standardization, Geneva, Switzerland. 2014. <https://www.iso.org/standard/67257.html>
- [34] EN ISO 9015. Destructive tests on welds in metallic materials - Hardness testing. International Organization for Standardization, Geneva, Switzerland. 2016. <https://www.iso.org/standard/67257.html>
- [35] EN ISO 5178. Destructive tests on welds in metallic materials – Longitudinal tensile test on weld metal fusion welded joints. International Organization for Standardization, Geneva, Switzerland. 2019. <https://www.iso.org/standard/75738.html>
- [36] EN ISO 6892-1. Metallic materials - Tensile testing - Part 1: Method of test at room temperature. International Organization for Standardization, Geneva, Switzerland. 2016. <https://www.iso.org/standard/61856.html>
- [37] EN ISO 15792-1. Welding consumables – Test methods – Part 1: test methods for all-weld metal test specimens in steel, nickel and nickel alloys. International Organization for Standardization, Geneva, Switzerland. 2000. <https://www.iso.org/standard/29050.html>
- [38] Fortan, M., De Wilder, K., Debruyne, D., Rossi, B. Shear buckling of lean duplex stainless steel plate girders with non-rigid end posts. *Proceedings of the 8th International Conference on Steel and Aluminium Structures 2016*. Hong Kong, China. 2016.
- [39] Sutton, M. A., Orteu, J.-J., Schreier, H. W. *Image Correlation for Shape, Motion and Deformation Measurements: Basic Concepts, Theory and Applications*. 2009.
- [40] MatchID www.matchid.eu
- [41] CloudCompare (version 2.8.1) [GPL software]. Retrieved from <http://www.cloudcompare.org/>. 2017
- [42] European Committee for Standardization (CEN), Eurocode 0: Basis of structural design, EN 1990:2002.
- [43] Afshan, S., Francis, P., Baddoo, N. R., Gardner, L. Reliability analysis of structural stainless steel design provisions. *Journal of Constructional Steel Research*, 114, 293-304, 2015.

- 1 [44] AISC Design Guide 27: Structural Stainless Steel. American Institute of Steel Construction, 2013.